On the use of numerical diffusive terms in weakly-compressible SPH schemes

M. Antuono
CNR-INSEAN
Rome, Italy

A. Colagrossi
CESOS
NTNU, Trondheim, Norway

S. Marrone
CNR-INSEAN
Rome, Italy

***Abstract*—An in-depth discussion on the use of numerical diffusive terms in SPH models has been performed. These terms are generally added inside the continuity equation in order to reduce the spurious numerical noise that affects the density and pressure fields in weakly-compressible SPH schemes. Specific focus has been given to the theoretical analysis of the diffusive term structure and to the choice of the integration scheme and Courant-Friedrick-Lewy number. The most widespread formulations, that is, those by Ferrari et al. [1], Molteni & Colagrossi [2] and Antuono et al. [3], have been studied in details, highlighting the main benefits and drawbacks.**

I. Introduction

In the SPH literature, two principal approaches are adopted to model liquids: one is based on the smoothing of the Navier-Stokes equations and on the solution of a Poisson equation for the pressure field, the other relies on the assumption that the fluid is weakly-compressible and barotropic.

From a numerical point of view, the main differences between the weakly-compressible and incompressible approaches is that the former requires small time steps constrained by the speed of sound, while the later needs to solve an algebraic system with a sparse matrix, allowing for larger time steps but rather complex for an efficient parallelization. Further, weakly-compressible schemes are generally more suited for free-surface flows since the boundary condition along the free surface is implicitly satisfied (see, for example, Colagrossi et al. [4]) and this avoids an explicit detection of the free surface during the flow evolution. The latter issue can be critical in 3D simulations of violent flows since the Poisson equation may strongly depend on the free surface configuration and small errors in the free-surface detection can lead to different flow dynamics.

Unfortunately, the weakly-compressibility schemes have as a major drawback the generation of spurious numerical oscillation in the pressure and density fields. Over the years, different solutions have been proposed to remove/reduce the spurious numerical noise that affect the pressure field in SPH model. Among them, one is to use proper diffusive terms. For example, Ferrari et al. [1] used a Rusanov flux and built a numerical diffusive term to be added inside the continuity equation. This helped reduce the numerical noise inside the density field and, consequently, inside the pressure field through the state equation (we recall that the fluid is assumed to be barotropic). The use of a numerical diffusive term inside the continuity equation has been also proposed by Molteni & Colagrossi [2]. Their term gave good results but, unfortunately, was inconsistent with the hydrostatic solution. The authors avoided this issue by introducing a threshold density so that the diffusive term only worked when the pressure field exceeded the hydrostatic field. Unfortunately, this strategy led to a drastic reduction of the diffusive term action. To go round this issue, Antuono et al. [3] proposed a correction to the diffusive term of Molteni & Colagrossi [2]. This proved to be compatible with the hydrostatic solution and to properly smooth out the numerical spurious oscillations from the pressure and density fields.

The aim of the present work is to shed light on the use of numerical diffusive terms in SPH. Specifically, we focus on the diffusive term of Ferrari et al. [1], Molteni & Colagrossi [2] and Antuono et al. [3] and show their benefits and drawbacks.

II. SPH scheme with numerical diffusive terms

In this section we study the general structure of a SPH scheme with a numerical diffusive term inside the continuity equation. Specifically, we assume the fluid to be weakly-compressible and barotropic. Under these hypotheses, the density variations are small and it is possible to linearize the state equation in the neighborhood of the reference density value to get a linear dependence of the pressure on the density field. Finally, the artificial viscous term by Monaghan & Gingold [5] is added inside the momentum equation for stability reasons. In any case, we underline that the theoretical analysis on the role of the diffusive term is completely general and can be applied to SPH schemes with different features.

Under the hypotheses above, the governing equations for the SPH scheme at hand are:

$$\begin{cases} \dfrac{D\rho_i}{Dt} = -\rho_i \displaystyle\sum_j (\boldsymbol{u}_j - \boldsymbol{u}_i)\cdot\nabla_i W_{ij}\, V_j + \delta\, h\, c_0\, \mathcal{D}_i \\ \dfrac{D\boldsymbol{u}_i}{Dt} = -\dfrac{1}{\rho_i}\displaystyle\sum_j (p_j + p_i)\,\nabla_i W_{ij}\, V_j + \\ \qquad + \boldsymbol{f}_i + \alpha\, h\, c_0 \dfrac{\rho_0}{\rho_i}\displaystyle\sum_j \pi_{ij}\,\nabla_i W_{ij}\, V_j \\ \dfrac{D\boldsymbol{r}_i}{Dt} = \boldsymbol{u}_i \qquad\qquad p_i = c_0^2(\rho_i - \rho_0) \end{cases} \tag{1}$$

where ρ_i, V_i, p_i are respectively the density, the volume and the pressure of the $i-$particle while $\boldsymbol{r}_i$ and $\boldsymbol{u}_i$ are its position

and velocity. Here, W_{ij} is the kernel function and depends on $q = \|\boldsymbol{r}_j - \boldsymbol{r}_i\|/h$, ∇_i denotes the differentiation with respect to $\boldsymbol{r}_i$ and $\boldsymbol{f}_i$ is the body force at the position $\boldsymbol{r}_i$. Finally, symbols ρ_0 and c_0 indicate the density along the free surface (which is the reference value for the density field) and the sound velocity (assumed to be constant). For computational reason, it is common practice in the weakly-compressible SPH solvers not to use the physical sound velocity but, conversely, to impose c_0 to be at least one order of magnitude greater than the maximum flow velocity, that is, $c_0 \geq 10 \max_i \boldsymbol{u}_i$. As pointed by Monaghan [7], this assumption ensures the density variation to keep below 1%.

In this scheme, the diffusive term is briefly indicated by $\mathcal{D}_i$ and has the dimension of the Laplacian of ρ. The coefficient δ is dimensionless and is used to control the order of magnitude of the dispersive term. For what concerns the artificial viscous term, the same role is played by the dimensionless parameter α. The argument of the summation is:

$$\pi_{ij} = \frac{(\boldsymbol{u}_j - \boldsymbol{u}_i) \cdot \boldsymbol{r}_{ji}}{\|\boldsymbol{r}_{ji}\|^2} \tag{2}$$

where $\boldsymbol{r}_{ji} = \boldsymbol{r}_j - \boldsymbol{r}_i$.

For the analysis which follows, it is useful to study the convergence of the pressure gradient operator in (1). Using the results of Colagrossi et al. [4] on the smoothed SPH operators, we can rewrite it as follows:

$$\sum_j (p_j + p_i)\, \nabla_i W_{ij}\, V_j = \sum_j (p_j - p_i)\, \nabla_i W_{ij}\, V_j + 2\, p_1 \sum_j \nabla_i W_{ij}\, V_j = \Gamma_i\, \nabla p_i + 2\, p_i\, \nabla\Gamma_i + O(h)\,, \tag{3}$$

where $\Gamma_i = \sum_j W_{ij} V_j$ and $\nabla\Gamma_i = \sum_j \nabla_i W_{ij} V_j$. As widely discussed in Colagrossi et al. [4], $\Gamma_i \simeq 1$ and $\nabla\Gamma_i \simeq 0$ inside the fluid domain. On the contrary, near the free surface Γ_i is no more constant and $\nabla\Gamma_i$ points inward the fluid domain and diverges like $1/h$. In this case, the convergence of the differential operator is ensured by assigning $p = 0$ along the free surface. Because of (3), the overall contribution to the momentum equation is:

$$\frac{D\boldsymbol{u}_i}{Dt} = -\frac{\Gamma_i}{\rho_i} \nabla p_i - \frac{2\, p_i}{\rho_i} \nabla\Gamma_i + \ldots \tag{4}$$

The last term in the right-hand side of (4) plays a relevant role when the diffusive term is added into the continuity equation. This is analyzed in the following section.

A. Diffusive terms

In the SPH literature, different diffusive terms have been defined. Generally, they can be reduced to the following structure:

$$\mathcal{D}_i = 2 \sum_j \psi_{ji}\, \frac{\boldsymbol{r}_{ji} \cdot \nabla_i W_{ij}}{\|\boldsymbol{r}_{ji}\|^2}\, V_j \tag{5}$$

where ψ_{ji} changes according to the specific formulation at hand and has the physical dimension of the density. In order to be a diffusive term, the expression in (5) has to approximate even derivatives of the density/pressure field. Further, For consistency with the global equation of the mass conservation, the diffusive term must satisfy:

$$\sum_i \mathcal{D}_i V_i = 0 \qquad \Leftrightarrow \qquad \psi_{ji} = -\psi_{ij}\,. \tag{6}$$

The simplest approach to artificial diffusion in SPH is that of Molteni & Colagrossi [2] who added the Laplacian of the density field inside the continuity equation. This is equivalent to choose:

$$\psi_{ji}^{Mol} = \rho_j - \rho_i \tag{7}$$

As shown in Antuono et al. [3], the use of (7) leads to:

$$\mathcal{D}_i^{Mol} = 2\, \nabla\rho_i \cdot \nabla\Gamma_i + \Gamma_i\, \nabla^2\rho_i + O(h)\,. \tag{8}$$

The second term in the right-hand side of (8) contains second-order derivatives and, therefore, represents a diffusive term. Conversely, the first term on the right-hand side is a nonlinear first-order differential operator and is negligible inside the fluid domain since $\nabla\Gamma_i \simeq 0$. On the contrary, $\nabla\Gamma_i$ is different from zero near the free surface and points inwards the fluid region. Since $\rho = 0$ out of the fluid, the density gradient points in the same direction and, therefore, $\nabla\rho_i \cdot \nabla\Gamma_i$ gives a positive contribution into the continuity equation. This leads to an increase of the density which corresponds (through the state equation) to an increase of the pressure field along the free surface. Finally, this implies that the term $(-p_i \nabla\Gamma_i)$ in (4) is no more zero and acts as a force directed outside the fluid body. Because of this phenomenon, particles start moving upward and cannot stand the hydrostatic solution.

A correction to the formula of Molteni & Colagrossi [2] has been proposed by Antuono et al. [3]. This formula is convergent all over the fluid domain, preserves exactly the conservation of mass and satisfies the hydrostatic solution. It reads:

$$\psi_{ji}^{An} = \left\{ \left(\rho_j - \rho_i\right) - \frac{1}{2} \left(\langle\nabla\rho\rangle_j^L + \langle\nabla\rho\rangle_i^L \right) \cdot \boldsymbol{r}_{ji} \right\} \tag{9}$$

Symbol $\langle\nabla\rho\rangle_i^L$ indicates the renormalized density gradient [8].

Another interesting approach to diffusion has been derived by Ferrari et al. [1] basing on a Rusanof flux. Assuming that the sound velocity is constant, their diffusive term reduces to:

$$\psi_{ji}^{Fe} = \frac{(\rho_j - \rho_i)}{2\, h}\, \|\boldsymbol{r}_{ji}\|\,. \tag{10}$$

Remarkably, the SPH scheme defined by Ferrari et al. [1] does not need any tuning of δ (which is set equal to 1) nor any artificial viscosity to stabilize the scheme. Notwithstanding this, such a term still leads to a positive contribution inside the continuity equation which makes impossible the attainment of the hydrostatic solution. This is proved in the following sections along with an accurate analysis of the diffusive term proposed by Ferrari et al. [1] and by Antuono et al [3].

III. Convergence of the diffusive operators

Here we deal with the convergence of the diffusive terms described in Section II-A. To simplify the discussion, we make an analysis at the continuous level substituting the summations over the fluid particles with integrals over the kernel domain Ω. In this context, we denote by $\boldsymbol{r}$ and $\boldsymbol{r'}$ two points in the fluid domain. All the quantities evaluated at $\boldsymbol{r'}$ are indicated through the superscript "prime" (i.e., f' indicates $f(\boldsymbol{r'})$). For the ease of the notation, we also define $\boldsymbol{q} = (\boldsymbol{r'} - \boldsymbol{r})/h$ and $q = \|\boldsymbol{q}\|$ while the subscripts k, l, m, n denote the components of vectors/tensors. As a consequence, the kernel gradient can be rewritten as follows:

$$W = W(q) \qquad \Rightarrow \qquad \nabla W = -\frac{1}{h}\frac{\boldsymbol{q}}{q}\frac{\partial W}{\partial q}, \tag{11}$$

and the structure of diffusive term in (5) becomes:

$$\mathcal{D} = -\frac{2}{h^2}\int_\Omega \frac{\psi}{q}\frac{\partial W}{\partial q}\,dV' \tag{12}$$

We first consider the expression by Ferrari et al. [1]. Using a Taylor expansion, we obtain:

$$\mathcal{D}^{Fe} = \nabla\rho\cdot\int_\Omega q\,\nabla W\,dV' + \frac{1}{2}\,\mathbb{H}(\rho) : \int_\Omega q\,(\boldsymbol{r'}-\boldsymbol{r})\otimes\nabla W\,dV' + O(h)\,,$$

where $\mathbb{H}$ is the Hessian of ρ. For symmetry reasons, the first term on the right-hand side is null inside the fluid domain while is different from zero near the free surface and is directed inwards the fluid region. Similarly to the term $\nabla\rho\cdot\nabla\Gamma$ in equation (8), this leads to a positive contribution inside the continuity equation and implies the impossibility to attain the hydrostatic solution.

A similar analysis proves that the diffusive term by Antuono et al. [3] converges to zero for h going to zero. Its main contributions are:

$$\begin{aligned}\mathcal{D}^{An} \;=\; & \frac{h}{6}\left(\frac{\partial^3\rho}{\partial r_k\partial r_l\partial r_m}\right)\int_\Omega \frac{q_k\,q_l\,q_m}{q}\frac{\partial W}{\partial q}\,dV' \;+ \\ & +\; \frac{h^2}{12}\left(\frac{\partial^4\rho}{\partial r_k\partial r_l\partial r_m\partial r_n}\right)\int_\Omega \frac{q_k\,q_l\,q_m\,q_n}{q}\frac{\partial W}{\partial q}\,dV' + O(h^3)\end{aligned} \tag{13}$$

where $q_k = (r'_k - r_k)/h$ is the $k-$th component of $\boldsymbol{q}$. For symmetry reasons, the first term in the right-hand side is null inside the fluid domain. On the contrary, near the free surface it is generally different from zero but keeps very small. Note that the diffusive term has no influence on the hydrostatic solution. In fact, since the state equation of system (1) is linear, the hydrostatic solution predicts a density field that is linear as well. Consequently, this implies $\mathcal{D}^{An} = 0$.

The presence of third- and fourth-order derivatives in (13) ensures that the diffusive term acts only when short-scale variations/fluctuations of the density field occur. As a consequence, it smooths out the spurious numerical high-frequency oscillations inside the pressure field without affecting the actual solution.

A. Linear stability analysis

Here we provide the one-dimensional linear stability analysis for the SPH scheme with the diffusive term proposed by Antuono et al. [3]. This analysis is performed at the continuous level, that is, using the continuous differential operators which are approximated by the discrete summations in system (1). To do this, we neglect the action of the free surface and take the limit for h going to zero. Under these hypotheses, the convergence of the SPH differential operators is given by Español & Revenga [9]. These allow rewriting system (1) into the following continuous form:

$$\begin{cases} \dfrac{D\rho}{Dt} \;=\; -\rho\,\nabla\cdot\boldsymbol{u} \;+\; \delta\,h\,c_0\,\mathcal{D}\,, \\ \dfrac{D\boldsymbol{u}}{Dt} \;=\; -\dfrac{\nabla p}{\rho} \;+\; 2\,\nu\,\nabla(\nabla\cdot\boldsymbol{u}) \;+\; \nu\,\nabla^2\boldsymbol{u} \\ p \;=\; c_0^2\,(\rho-\rho_0)\,. \end{cases} \tag{14}$$

which corresponds to a weakly-compressible version of the Navier-Stokes equations with a diffusive term inside the continuity equations. Let us consider the linearized one-dimensional form of system (14) and use the diffusive term of Antuono et al. [3]. In one dimension $\nu = \alpha h c_0/6$ (see, for example, Monaghan & Gingold [5]) while the diffusive term can be rewritten as:

$$\mathcal{D}^{An} \;=\; -h^2\,B\,\frac{\mathrm{d}^4\rho}{\mathrm{d}x^4} \tag{15}$$

where the parameter B is obtained by rewriting the second integral term inside equation (13) in one dimension, that is:

$$\mathbb{B}_{ijkp} = \int_\Omega \frac{q_i\,q_j\,q_k\,q_p}{q}\frac{\partial W}{\partial q}\,dV' \quad\Rightarrow\quad B = \int_\Omega q\,\frac{\partial W}{\partial q}\,dV'\,. \tag{16}$$

Note that B depends on the specific kernel function used. Then, system (14) becomes:

$$\begin{cases} \rho_t \;+\; \rho_0\,u_x \;+\; \delta\,h^3\,c_0\,B\,\rho_{xxxx} \;=\; 0 \\ u_t \;+\; \dfrac{c_0^2}{\rho_0}\,\rho_x \;-\; \dfrac{\alpha\,h\,c_0}{2}\,u_{xx} \;=\; 0 \end{cases} \tag{17}$$

Let us assume:

$$\rho = \rho_0 \;+\; R\,e^{i\,k\,(x-c\,t)} + c.c. \qquad u = U\,e^{i\,k\,(x-c\,t)} + c.c. \tag{18}$$

where $c = a + i\,b$, $k = 2\,\pi/\lambda$ is the wave number and λ is the wave length. Now, substituting (18) in (17) and using the variable $\mu = k\,h$, we get two different regimes for the solution of the linearized equations. The first one is obtained when:

$$F(\mu) \;=\; 1 \;-\; \frac{\mu^2}{4}\left(\frac{\alpha}{2} \;-\; \mu^2\,B\,\delta\right)^2 \;\geq\; 0\,. \tag{19}$$

and gives:

$$a^{(\pm)} \;=\; \pm\,c_0\,\sqrt{F(\mu)} \qquad b^{(0)} \;=\; -\frac{\mu\,c_0}{2}\left(\frac{\alpha}{2} + \mu^2\,B\,\delta\right) \tag{20}$$

Conversely, when $F(\mu) < 0$, we get the second regime:

$$a^{(0)} = 0 \qquad b^{(\pm)} = c_0\,\left\{-\frac{\mu}{2}\left(\frac{\alpha}{2} + \mu^2\,B\,\delta\right) \pm \sqrt{-F(\mu)}\right\} \tag{21}$$

In this case, the correct damping rate is given by $b^{(+)}$ since $b^{(-)} \leq b^{(+)} \leq 0$.

Since b is negative in both the regimes, this ensures the stability of the δ-SPH scheme. Figure 1 displays a/c_0 (dashed line) and b/c_0 (solid line) as functions of μ for $\alpha = 0.01$, $\delta = 1.0$ and $B = 1/8$ (Gaussian kernel). The damping coefficient b is strictly decreasing in the first regime, reaches a minimum at the boundary with the second regime and, then, become an increasing function of μ (here we refer to $b^{(+)}$). This implies that the occurrence of the second regime is associated with a reduced damping of the higher frequencies (or equivalently, with a reduced damping of the shorter wave lengths). For this reason, an optimal choice for δ is that ensuring the occurrence of the first regime, that is, the fulfillment of the condition (19). This corresponds to:

$$\frac{1}{B\mu^2}\left(\frac{\alpha}{2}-\frac{2}{\mu}\right) \leq \delta \leq \frac{1}{B\mu^2}\left(\frac{\alpha}{2}+\frac{2}{\mu}\right). \tag{22}$$

Now, we have to define the range of variability of μ. Note that the minimum length of the spurious oscillations in the SPH framework is that corresponding to a sawtooth profile, that is, $\lambda = 2\Delta x$. Then, the maximum value for μ is given by $\mu_0 = \pi(h/\Delta x)$. For the Gaussian kernel $h/\Delta x = 4/3$ and, therefore, $\mu_0 = 4\pi/3$. Since the upper bound in (22) is a strictly decreasing function of μ while the lower bound has a maximum at $\mu = 6/\alpha$, the expression (22) can be modified to get a *sufficient* condition for the fulfillment of the condition (19) for all $\mu \in [0, \mu_0]$:

$$\frac{1}{B}\left(\frac{\alpha}{6}\right)^3 \leq \delta \leq \frac{1}{B\mu_0^2}\left(\frac{\alpha}{2}+\frac{2}{\mu_0}\right). \tag{23}$$

Note that the expression above is valid for $\alpha < 12/\mu_0$ otherwise the lower bound is greater than the upper bound. For $\alpha = 0$ and $B = 1/8$ (Gaussian kernel), relation (23) simply becomes $\delta \leq 0.21$. Then, to guarantee the occurrence of the first regime, we fix $\delta = 0.2$ in all the numerical simulations that implement $\mathcal{D}^{An}$.

It is interesting to repeat the analysis above for $\delta = 0$, that is, when only the viscous term is included inside the SPH scheme. In this case, the linear stability analysis still confirms that the solution is stable for each choice of α. Specifically, the condition (19) is surely satisfied when:

$$0 < \alpha < \frac{4}{\mu_0}. \tag{24}$$

Similarly to the analysis made for $\delta \neq 0$, values of α out of the interval in (24) lead the solution in the region of slow damping. Before proceeding to the analysis, it is useful to do a final remark. The range of variability of α in (24) is more narrow than the case with diffusion (for which $0 < \alpha < 12/\mu_0$). This means that the use of the diffusive term allows for a more efficient action of the viscosity against the numerical spurious oscillations.

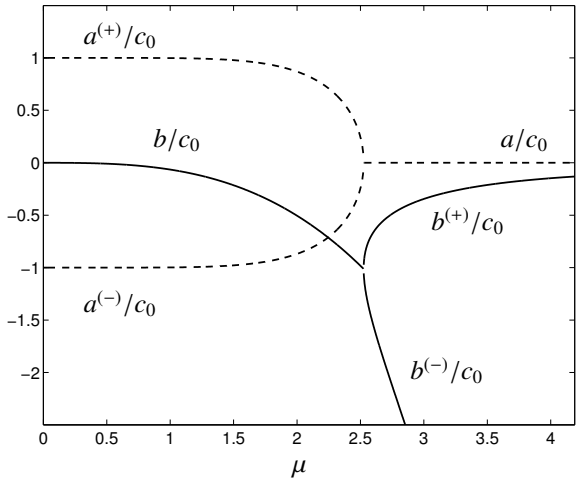

Fig. 1. sketch of the regimes predicted by the one-dimensional linear stability analysis: a/c_0 (dashed line) and b/c_0 (solid line) for $\alpha = 0.01, \delta = 1.0$ and $B = 1/8$ (Gaussian kernel).

IV. Integration Scheme

Before proceeding to the numerical analysis, it is important to briefly describe the integration scheme. We tested both a third-order TVD Runge-Kutta scheme (see, for example, Gottlieb & Shu [10]) and a classic fourth-order Runge-Kutta scheme. We found that the accuracy of these schemes was practically equivalent even if the fourth-order Runge-Kutta scheme proved to be faster than the TVD scheme because of its higher Courant-Friedrick-Lewy number. For this reason, the fourth-order Runge-Kutta scheme has been used for the simulations that implement the diffusive term of Antuono et al. [3]. On the contrary, to follow exactly the integration scheme proposed in Ferrari et al. [1], we used the third-order TVD Runge-Kutta scheme for simulations with $\mathcal{D}^{Fe}$.

For what concerns the fourth-order Runge-Kutta scheme, the diffusive term can be added directly in all the sub-steps. However, the expense of re-evaluating the diffusive term at every stage of the scheme may be substantial. Then, Jameson et al. [11] proposed a faster scheme to integrate systems with artificial diffusive/dissipative terms. First, we rewrite system (1) as $D\boldsymbol{w}/Dt = \boldsymbol{Q}(\boldsymbol{w}) + \boldsymbol{D}(\boldsymbol{w})$ where $\boldsymbol{D}$ contains only the diffusive term. Then, this is integrated by using a fourth-order Runge-Kutta scheme with "frozen" diffusion, that is:

$$\left\{\begin{array}{l} \boldsymbol{w}^{(0)} = \boldsymbol{w}^n \\ \boldsymbol{w}^{(1)} = \boldsymbol{w}^{(0)} + \boldsymbol{D}(\boldsymbol{w}^{(0)})\,\Delta t/2 + \boldsymbol{Q}(\boldsymbol{w}^{(0)})\,\Delta t/2 \\ \boldsymbol{w}^{(2)} = \boldsymbol{w}^{(0)} + \boldsymbol{D}(\boldsymbol{w}^{(0)})\,\Delta t/2 + \boldsymbol{Q}(\boldsymbol{w}^{(1)})\,\Delta t/2 \\ \boldsymbol{w}^{(3)} = \boldsymbol{w}^{(0)} + \boldsymbol{D}(\boldsymbol{w}^{(0)})\,\Delta t + \boldsymbol{Q}(\boldsymbol{w}^{(2)})\,\Delta t \\ \boldsymbol{w}^{(4)} = \boldsymbol{w}^{(0)} + \boldsymbol{D}(\boldsymbol{w}^{(0)})\,\Delta t + \\ \qquad + [\,\boldsymbol{Q}(\boldsymbol{w}^{(0)}) + 2\boldsymbol{Q}(\boldsymbol{w}^{(1)}) + 2\boldsymbol{Q}(\boldsymbol{w}^{(2)}) + \boldsymbol{Q}(\boldsymbol{w}^{(3)})\,]\,\Delta t/6 \\ \boldsymbol{w}^{n+1} = \boldsymbol{w}^{(4)}. \end{array}\right. \tag{25}$$

Jameson et al. [11] proved this scheme to be robust and reliable. The integration of the artificial diffusive term is less accurate then the classic fourth-order Runge-Kutta scheme but,

in any case, this can be regarded as a minor issue since $\mathcal{D}$ does not represent a physical diffusion phenomenon.

The last part of the analysis is devoted to the definition of a proper Courant-Friedrick-Lewy number (*CFL* hereinafter) for the integration scheme described in (25). Using equations (13) and (16), we can rewrite the diffusive term as follows:

$$\mathcal{D}_i^{An} = \frac{h^2}{12}\,\mathbb{B}_{jkpq}\left(\frac{\partial^4 \rho_i}{\partial r_j \partial r_k \partial r_p \partial r_q}\right), \qquad (26)$$

where i is the particle index while j, k, p, q are the indexes of the spatial coordinates. Substituting (26) inside the continuity equation and comparing with $D\rho_i/Dt$ it follows:

$$\Delta t \leq CFL^{(diff)}\,\frac{h}{\delta\, c_0}\,. \qquad (27)$$

This means that the time step should decrease when the diffusive coefficient increases. For a fourth-order Runge-Kutta scheme with a Gaussian kernel we heuristically found $CFL^{(diff)} = 0.44$. The global *CFL* should also account for the artificial viscosity and for the particle acceleration $\boldsymbol{a}_i$. The time-step bounds deriving from these terms have been modeled following the works of Monaghan & Kos [12] and Morris et al. [13]. They depend on the specific integration scheme very weakly and are given by the following bounds:

$$\Delta t \leq 0.125\,\frac{h^2}{\nu} \qquad \Delta t \leq 0.25\,\min_i \sqrt{\frac{h}{\|\boldsymbol{a}_i\|}}\,, \qquad (28)$$

where, according to Monaghan [7], $\nu = \alpha h c_0/(2n+4)$ is the kinematic viscosity of the SPH scheme (n is the spatial dimension). Finally, the advective/acoustic component of system (1) should be accounted for. For a fourth-order Runge-Kutta scheme with a Gaussian kernel we heuristically found:

$$\Delta t \leq 2.2\,\min_i\left(\frac{h}{c_0 + \|\boldsymbol{u}_i\| + h\max_j \pi_{ij}}\right). \qquad (29)$$

The global *CFL* is given by the minimum over all the bounds above.

V. Test cases

In the following sections we provide some numerical simulations that highlight the main features of the diffusive terms mentioned before. Because of the resemblance of the diffusive term of Molteni & Colagrossi [2] with that of Ferrari et al. [1], hereinafter we just consider the latter one.

In all the numerical simulations that follow the solid boundaries have been modeled through the fixed ghost particle technique (see Marrone et al. [14]) and a free-slip condition has been imposed. A renormalized Gaussian kernel has been adopted (see, for example, Landrini et al. [15]).

A. Hydrostatic solution

In the present section we deal with a simple hydrostatic problem: a two-dimensional tank is partially filled with water at rest. Here, L is the tank length and H is the filling height. Figure (2) displays the comparison between the SPH with the diffusive term of Ferrari et al. [1] and with the diffusive term of Antuono et al. [3] for two spatial resolutions. As expected, in the former case the fluid particles tend to move upward because of the inaccuracy of the diffusive term close to the free surface and the hydrostatic solution is completely destroyed. This behavior still persists using a finer resolution even if it slightly decreases in intensity. Conversely, the use of the diffusive term of Antuono et al. [3] does not alter the correct hydrostatic solution.

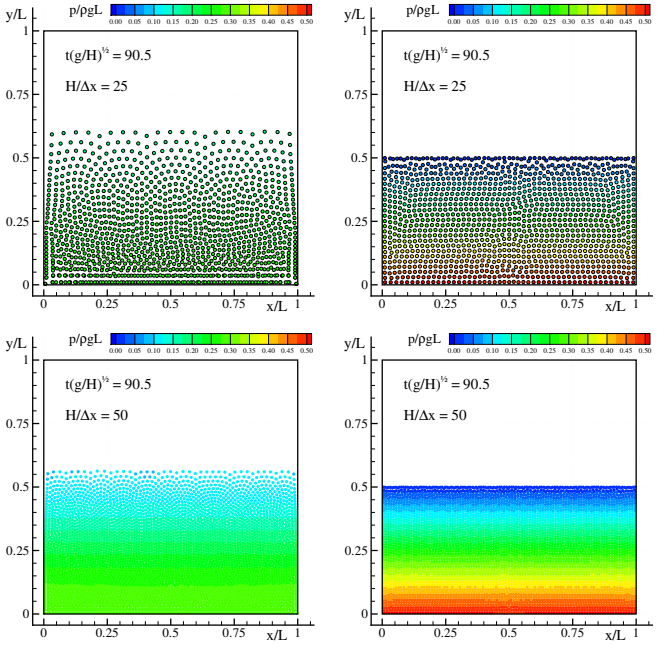

Fig. 2. hydrostatic solution. Left panels: SPH with the diffusive term of Ferrari et al. [1]. Right panels: SPH with the diffusive term of Antuono et al. [3].

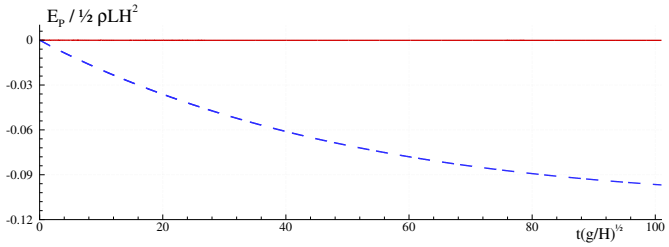

Fig. 3. hydrostatic solution. Evolution of the potential energy as predicted by the SPH scheme with the diffusive term of Ferrari et al. [1] (dashed line) and with the diffusive term of Antuono et al. [3].

A further prove of the unphysical action of the diffusive term of Ferrari et al. [1] is given in figure 3 where the evolution of the potential energy is displayed. In hydrostatic conditions, the potential energy should be conserved since no motion should occur. On the contrary, the diffusive term of Ferrari et al. [1] leads to a rapid decrease of the initial energy value.

The unphysical motion of the free surface also affects those problems characterized by a slow particle motion and a long-time dynamics as, for example, sloshing problems and gravity wave propagation. Conversely, for more energetic events and

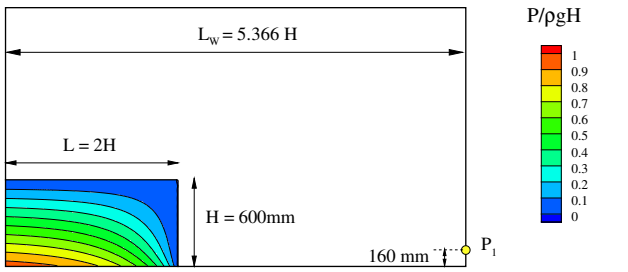

Fig. 4. sketch of the dam-break problem described in Buchner et al. [16]. Symbol P_1 indicate the pressure probe at the right wall.

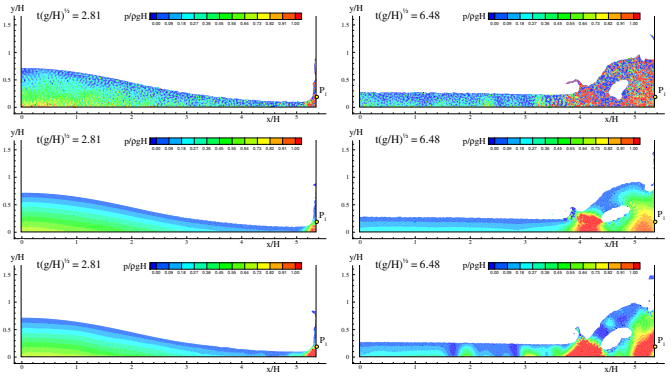

Fig. 5. snapshots of the evolution for the dam break problem ($\alpha = 0$). Top panels: SPH without diffusion. Middle panels: SPH with the diffusive term of Ferrari et al. [1]. Bottom panels: SPH with the diffusive term of Antuono et al. [3].

short-time dynamics (as, for example, water jets and impacts), the influence of the spurious terms close to the free surface is much smaller. This is highlighted in the next test case.

B. Dam break

Here we consider the experimental campaign of Buchner [16] on dam-break problems. A sketch is displayed in figure 4: a reservoir is placed at the left side of a rectangular basin with water at rest. Then, the right wall of the reservoir is suddenly removed and the water starts moving until it impacts against the right wall of the basin. Along the wall, a probe (indicated by P_1) records the pressure signal. The sketch in figure 4 displays the pressure field just after the right wall of the reservoir has been removed.

The simulations have been first performed with $\alpha = 0$ and implementing the diffusive term of Ferrari et al. [1] and of Antuono et al. [3]. Some snapshots of the evolution are displayed in figure 5 along with the standard SPH (that is, the SPH model without diffusion). The impact against the right wall occurs at about $t \simeq 2.81\sqrt{H/g}$ where H is the initial water height. Then, a plunging breaking wave is generated and collapses at about $t \simeq 6.48\sqrt{H/g}$. These plots clearly prove that the use of a diffusive term drastically reduced the high-frequency spurious noise that affects the pressure field. In this case, the diffusive term of Ferrari et al. [1] gives the best results since, being a second order operator, smooths out the largest

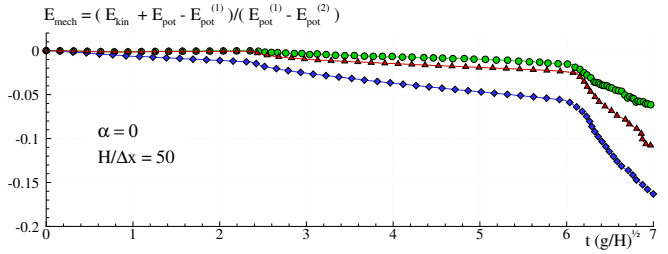

Fig. 6. evolution of the mechanical energy for the dam break problem with $\alpha = 0$. SPH without diffusion (○), SPH with the diffusive term of Ferrari et al. [1] (⋄), SPH with the diffusive term of Antuono et al. [3] (△).

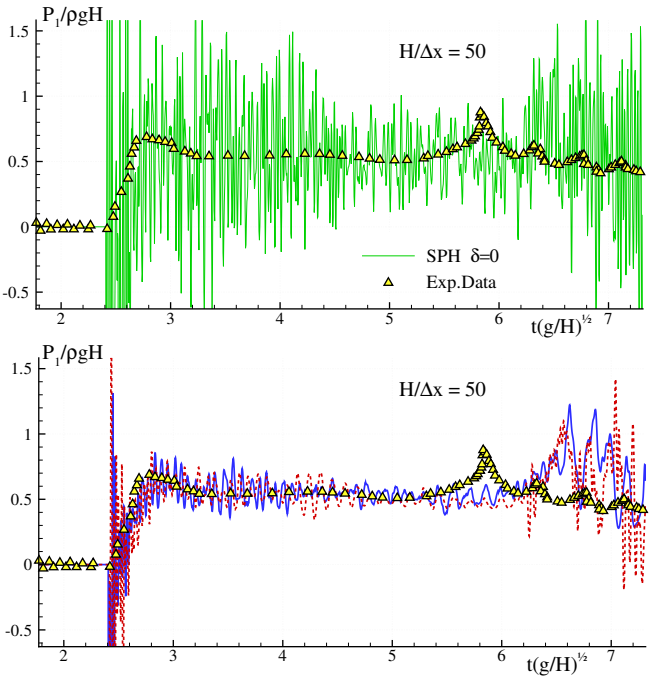

Fig. 7. pressure signal at probe P_1. Comparison between the experimental data (△), the SPH without diffusive term (top panel, solid line), the SPH with the diffusive term of Ferrari et al. [1] (bottom panel, solid line) and with the diffusive term of Antuono et al. [3] (bottom panel, dashed line).

part of the spurious sound waves which propagate inside the fluid. Conversely, the diffusive term of Antuono et al. [3] still displays some traveling sound waves after the impact at the right wall (see the lower right panel of figure 5).

In figure 6 the evolution of the mechanical energy (that is, potential plus kinetic energy) is shown. Because of the weakly-compressibility assumption, part of the mechanical energy is converted in internal energy during the impact and the subsequent splash-up processes. The standard SPH scheme and the SPH with the diffusive term of Antuono et al. [3] show a good agreement and a good conservation of the mechanical energy. Conversely, the SPH with the diffusive term of Ferrari et al. [1] displays a larger action of the weakly-compressibility and a consequent larger damping of the mechanical energy.

Figure 7 displays the pressure signal at the probe P_1 and the comparison with the experimental data of Buchner [16]. Differently from the results shown in Marrone et al. [14] where

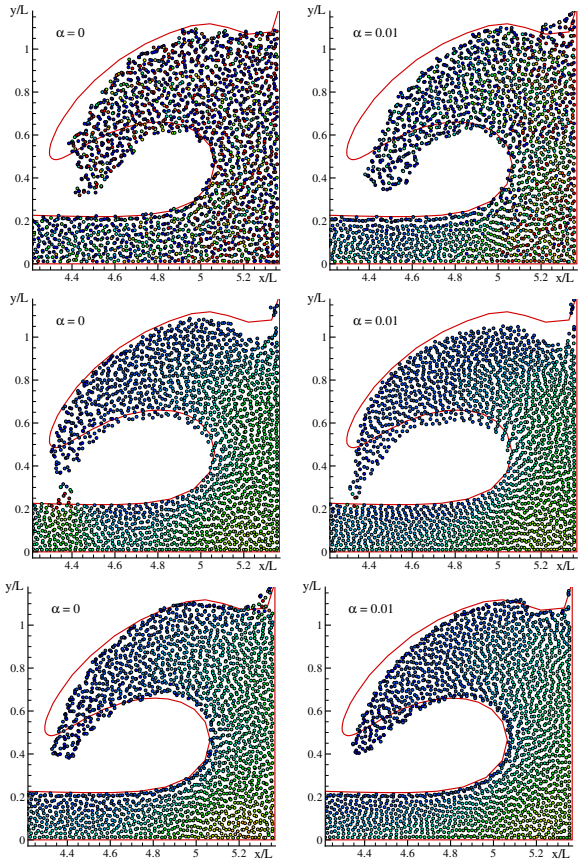

Fig. 8. snapshots of the evolution for the dam break problem at $t = 6\sqrt{H/g}$ for $\alpha = 0$ (left panels) and $\alpha = 0.01$ (right panels). Solid lines indicate the free surface predicted by the BEM solver. Top panels: SPH without diffusion. Middle panels: SPH with the diffusive term of Ferrari et al. [1]. Bottom panels: SPH with the diffusive term of Antuono et al. [3].

the signals were averaged over the probe area, here we provide the local numerical solution at $(x/H, y/H) = (5.366, 0.266)$ (i.e., at the probe position). The pressure signal predicted by the standard SPH is practically destroyed by the high-frequency spurious oscillations (see top panel of figure 7). Conversely, the signal is recovered when the diffusive terms are introduced inside the continuity equation. As expected, the diffusive term of Ferrari et al. [1] (second-order differential operator) tends to smooth out lower frequencies with respect to that of Antuono et al. [3] (fourth-order differential operator). In any case, the pressure signals are comparable and show a good agreement with the experiments. Specifically, the match is very good up to $t = 5.7\sqrt{H/g}$. After this time, the plunging wave is closing a cavity that in the experiments is filled with air. Thus, the experimental pressure probe starts recording the influence of the air-cushioning before the actual closure of the cavity (see [6]). Conversely, in the present mono-fluid simulations, the pressure increase is predicted with a small delay, occurring only when the plunging wave actually closes the cavity at $t = 6\sqrt{H/g}$.

To complete the present analysis, we also inspected the influence of the artificial viscosity on the SPH simulations.

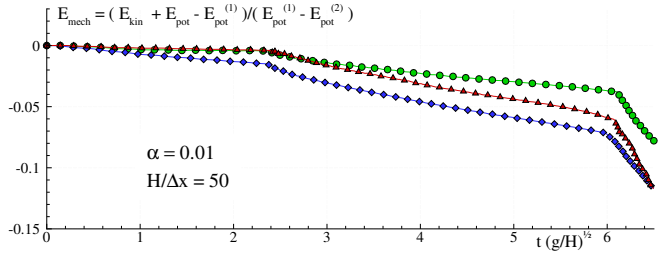

Fig. 9. evolution of the mechanical energy for the dam break problem with $\alpha = 0.01$. SPH without diffusion (○), SPH with the diffusive term of Ferrari et al. [1] (⋄), SPH with the diffusive term of Antuono et al. [3] (△).

Figure 8 displays a comparison between the SPH outputs with $\alpha = 0$ (no artificial viscosity) and $\alpha = 0.01$ during the generation of the plunging breaking wave. The action of the viscosity plays a major role in the standard SPH (upper panels) leading to a reduction of the spurious noise in the pressure field and a more regular shape of the free surface. For what concerns the diffusive SPH schemes (middle and bottom panels), the viscosity influence is less evident but, similarly to the previous case, it helps regularizing the free surface. All the free surface profiles have been compared with the potential solution obtained by using a Mixed Eulerian Lagrangian Boundary Element Method (BEM-MEL) [17] (solid lines in figure 8). The match generally improves when the diffusive terms are included in the SPH scheme and the viscosity seems not to alter the global shape of the plunging jet. As a final part of this analysis, we show the evolution of the mechanical energy with $\alpha = 0.01$ (figure 9). The overall behavior is similar to that highlighted in figure 6 with a faster damping of the mechanical energy because of the use of the artificial viscosity. During the earlies stages of the evolution, the SPH scheme with diffusive term of Antuono et al. [3] seems to better preserve the mechanical energy and shows a good match with the standard SPH scheme. Conversely, the SPH scheme with diffusive term of Ferrari et al. [1] displays the larger dissipation. Apart from these details, the use of a small artificial viscosity does not alter the overall behavior of the simulations and helps regularize the different SPH schemes.

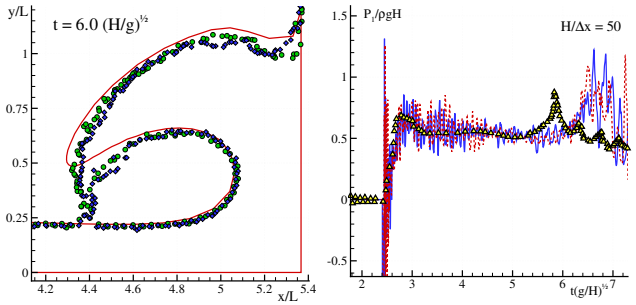

Fig. 10. dam break problem with $\alpha = 0$. Left: detail of the plunging wave as predicted by the BEM solver (solid line), by the SPH with the diffusive term of Ferrari et al. [1] (○) and with the diffusive term of Molteni and Colagrossi [2] (⋄, $\delta = 0.5$). Right: comparison between the experimental data (△), the SPH with the diffusive term of Ferrari et al. [1] (solid line) and with the diffusive term of Molteni and Colagrossi [2] (dashed line, $\delta = 0.5$).

Before concluding, we show the comparison between the SPH with the diffusive term of Molteni & Colagrossi [2] and the diffusive term of Ferrari et al. [1]. As already pointed out, these terms have the same structure, that is, they are both second-order differential operators. Comparing formulas (7) and (10), it turns out that they have the same order of magnitude if the diffusive term of Molteni & Colagrossi [2] is implemented with $\delta = 0.5$. Figure 10 displays the results obtained by using the SPH schemes that implement these diffusive terms. The left panel shows the plunging breaking wave and the comparison with the BEM-MEL solver while the right panel displays the comparison between the pressure signals at probe P_1 and the experiments. As expected, the diffusive terms of Molteni & Colagrossi [2] and Ferrari et al. [1] lead to results that are very similar. This further confirms the validity of the theoretical analysis provided in Section II-A and Section III.

VI. Conclusions

The theoretical analysis of the different numerical diffusive terms showed some inconsistencies in the formulations of Ferrari et al. [1] and Molteni & Colagrossi [2]. These are both incompatible with the hydrostatic solution and lead to an unphysical motion of the fluid particles. This issue also affects those problems characterized by a slow particle motion and a long-time dynamics as, for example, sloshing problems and gravity wave propagation. Conversely, the formulation proposed by Antuono et al. [3] proved to be consistent both in hydrostatic and dynamic conditions.

Apart from this, all formulations proved to be reliable and accurate when applied to problems characterized by energetic events and short-time dynamics (as, for example, water jets and impacts). In this context, the formulations of Ferrari et al. [1] and Molteni & Colagrossi [2] showed a stronger smoothing action on the pressure field than the formulation of Antuono et al. [3].

Acknowledgements

The Authors would like to thank Dr. Andrea Di Mascio for his useful comments and suggestions. This work was supported by the Centre of Excellence for Ship and Ocean Structures of NTNU Trondheim (Norway) within the “Violent Water-Vessel Interactions and Related Structural Loads”.

References

[1] A. Ferrari, M. Dumbser, E. F. Toro, A. Armanini, *A new 3D parallel SPH scheme for free-surface flows*, Computers & Fluids, **38**: 1203-1217, (2009).

[2] D. Molteni & A. Colagrossi, *A simple procedure to improve the pressure evaluation in hydrodynamic context using the SPH*, Computer Physics Communications, **180(6)**: 861–872, (2009).

[3] M. Antuono, A. Colagrossi, S. Marrone, D. Molteni *Free-surface flows solved by means of SPH schemes with numerical diffusive terms*, Computer Physics Communications, **181**: 532-549, (2010).

[4] A. Colagrossi, M. Antuono, D. Le Touzé, *Theoretical considerations on the free surface role in the SPH model*, Physical Review E, **79**/5, 056701: 1-13, (2009).

[5] J.J. Monaghan & R.A. Gingold, *Shock Simulation by the Particle Method SPH*, J. Comp. Phys., **52**, 374–389, (1983).

[6] A. Colagrossi and M. Landrini, Numerical Simulation of Interfacial Flows by Smoothed Particle Hydrodynamics, *Journal of Computational Physics*, **191**, 448–475, (2003).

[7] J.J. Monaghan, *Smoothed Particle Hydrodynamics*, Rep. Prog. Phys. **68**, 1703–1759, (2005).

[8] Randles, P.W. & Libersky, L.D., *Smoothed Particle Hydrodynamics: Some recent improvements and applications* Comput. Methods Appl. Mech. Engng., **139**, 375-408, (1996).

[9] P. Español & M. Revenga, *Smoothed dissipative particle dynamics*, Physical Review E, **67**, 026705 1–12, (2003).

[10] S. Gottlieb & C-W. Shu, *Total variation diminishing Runge-Kutta schemes*, Mathematics of Computation, **67**(221), 73-85, (1998).

[11] A. Jamenson, W. Schmidth, E. Turkel, *Numerical Solution of the Euler Equations by Finite Volume Methods Using Runge-Kutta Time-Stepping Schemes*, AIAA 14-th Fluid and Plasma Dynamics Conference, Palo Alto, CA, June 23-25 (1981).

[12] J.J. Monaghan, A. Kos, Solitary waves on a Cretan beach, J. Waterway, Port, Coastal and Ocean Engng. **125**, 145–154, (1999).

[13] J. P. Morris, P. J. Fox, Y. Zhu, *Modeling Low Reynolds Number Incompressible Flows Using SPH*, Journal of computational Physics, **136**, 214-226, (1997).

[14] S. Marrone, M. Antuono, A. Colagrossi, G. Colicchio, D. Le Touzé, G. Graziani, *δ-SPH model for simulating violent impact flows*, Comput. Methods Appl. Mech. Engrg., **200**, 1526-1542, (2011).

[15] M. Landrini, A. Colagrossi, M. Greco, M.P. Tulin, *Gridless simulations of splashing processes and near-shore bore propagation*, J. Fluid Mech. **591**, 183-213, (2007).

[16] B. Buchner, *Green Water on Ship-type Offshore Structures*, Ph.D. Thesis, Delft University of Technology, (2002).

[17] M. Greco, *A Two-dimensional Study of Green-Water Loading* PhD Thesis University of Trondheim, Norway, (2001).